UV-Radiation Response Proteins Reveal Undifferentiated Cutaneous Interfollicular Melanocytes with Hyperradiosensitivity to Differentiation at 0.05 Gy Radiotherapy Dose Fractions

Authors: Fessé, Per, Qvarnström, Fredrik, Nyman, Jan, Hermansson, Ingegerd, Ahlgren, Johan, et al.

Source: Radiation Research, 191(1) : 93-106

Published By: Radiation Research Society

URL: https://doi.org/10.1667/RR15078.1

RADIATION RESEARCH **191**, 93–106 (2019)
0033-7587/19 $15.00

DOI: 10.1667/RR15078.1

UV-Radiation Response Proteins Reveal Undifferentiated Cutaneous Interfollicular Melanocytes with Hyperradiosensitivity to Differentiation at 0.05 Gy Radiotherapy Dose Fractions

Per Fessé,[a,b,1] Fredrik Qvarnström,[b] Jan Nyman,[c] Ingegerd Hermansson,[c] Johan Ahlgren[d] and Ingela Turesson[b]

[a] *Centre for Research and Development, Uppsala University/Region Gävleborg, Gävle, Sweden;* [b] *Department of Immunology, Genetics and Pathology, Experimental and Clinical Oncology, Uppsala University, Uppsala, Sweden;* [c] *Department of Oncology, Institute of Clinical Sciences, Sahlgrenska Academy, University of Gothenburg, Gothenburg, Sweden; and* [d] *Department of Oncology, Faculty of Medicine and Health, Örebro University, Örebro Sweden*

Fessé, P., Qvarnström, F., Nyman, J., Hermansson, I., Ahlgren, J. and Turesson, I. UV-Radiation Response Proteins Reveal Undifferentiated Cutaneous Interfollicular Melanocytes with Hyperradiosensitivity to Differentiation at 0.05 Gy Radiotherapy Dose Fractions. *Radiat. Res.* 191, 93–106 (2019).

To date, the response activated in melanocytes by repeated genotoxic insults from radiotherapy has not been explored. We hypothesized that the molecular pathways involved in the response of melanocytes to ionizing radiation and ultraviolet radiation (UVR) are similar. Skin punch biopsies, not sun-exposed, were collected from prostate cancer patients before, as well as at 1 and 6.5 weeks after daily doses of 0.05–1.1 Gy. Interfollicular melanocytes were identified by ΔNp63- and eosin-periodic acid Schiff staining. Immunohistochemistry and immunofluorescence were performed to detect molecular markers of the melanocyte lineage. Melanocytes were negative for ΔNp63, and the number remained unchanged over the treatment period. At radiation doses as low as 0.05 Gy, melanocytes express higher protein levels of microphthalmia-associated transcription factor (MITF) and Bcl-2. Subsets of MITF- and Bcl-2-negative melanocytes were identified among interfollicular melanocytes in unexposed skin; the cell number in both subsets was reduced after irradiation in a way that indicates low-dose hyperradiosensitivity. A corresponding increase in MITF- and Bcl-2-positive cells was observed. PAX3 and SOX10 co-localized to some extent with MITF in unexposed skin, more so with radiation exposure. Low doses of ionizing radiation also intensified c-KIT and DCT staining. Nuclear p53 and p21 were undetectable in melanocytes. Apoptosis and proliferation could not be observed. In conclusion, undifferentiated interfollicular melanocytes were identified, and responded with differentiation in a hypersensitive manner at 0.05 Gy doses. Radioresistance regarding cell death was maintained up to fractionated doses of 1.1 Gy, applied for 7 weeks. The results suggest that the initial steps of melanin synthesis are common to ionizing radiation and UVR, and underline the importance of keratinocyte-melanocyte interaction behind hyperpigmentation and depigmentation to radiotherapy.

INTRODUCTION

In the treatment of cancer, the increasing use of intensity-modulated radiation therapy and volumetric-modulated arc therapy to escalate the dose to the tumor results in the exposure of large volumes of normal tissue to low and moderate doses of radiation. These radiotherapy techniques have increased the interest in understanding the DNA damage response and cellular outcome after irradiation at sub-therapeutic doses, particularly for cell types that respond with hypersensitivity to very low doses of ionizing radiation. In previously published clinical studies of the effects of radiation on skin samples, particularly keratinocytes, low-dose hypersensitivity was established using doses below 0.3 Gy for the following cellular end points (*1–4*): induction of DNA double-strand breaks (DSBs), growth arrest, apoptosis and rate of keratinocyte loss in the basal cell layer. The low-dose hypersensitivity, which was followed by induced radioresistance, persisted in epidermal keratinocytes for all measured effects over a radiotherapy course of 7 weeks, given daily dose fractions of 0.05–1.1 Gy. In this work, we present the response of melanocytes in the skin to ionizing radiation using the same clinical samples as in the previously reported work with keratinocytes.

Melanocytes are neural crest-derived, pigment-producing cells. In addition to their presence in hair follicles, cutaneous melanocytes in humans are present in the interfollicular epidermis, on the basement membrane of the epidermal-dermal junction. Approximately one interfollicular melanocyte is observed for every 5–6 basal keratinocytes. Upon exposure to ultraviolet radiation (UVR), melanin production in specialized organelles called

[1] Address for correspondence: Centre for Research and Development, Uppsala University/Region Gävleborg, Lassaretsvägen 1, Gävle, Gävleborg S80188, Sweden; email: per.fesse@regiongavleborg.se.

melanosomes results in skin pigmentation. The melanosomes are distributed as pigment granules through the tips of the dendrites of the melanocytes. These are able to reach all keratinocytes of the epidermis, creating a direct shield against UVR (*5, 6*).

Hyperpigmentation of the skin manifests not only as tanning after sun exposure, but also in other clinical situations, such as after inflammation and as a consequence of adrenal insufficiency (*7*). Hyperpigmentation and depigmentation occur frequently in radiotherapy and are often long-lasting in areas exposed to radiation. To the best of our knowledge, the mechanisms underlying these phenomena have not been explored. In contrast, the mechanisms regulating UVR-induced pigmentation have been investigated extensively, and novel regulatory pathways that highlight the interactions between keratinocytes and melanocytes were recently described elsewhere (*8, 9*).

Neural crest cells generate melanocyte precursor cells that are partially committed to the postnatal melanocyte lineage but remain undifferentiated. In adult human skin, the melanocyte precursor cells reside in the hair follicle bulge area and consist of two distinct cell populations: the melanocyte stem cells and their transit amplifying progeny, melanoblasts. Generally, melanocyte stem cells are quiescent, cycle slowly and function as a melanocyte reservoir. Upon appropriate stimulation, these immature cells are capable of regenerating mature melanocytes to maintain pigmentation during each hair cycle and replenish melanocytes of the interfollicular epidermis when necessary (*10–12*). Whether an independent and self-sufficient subset of melanocyte precursor cells exists in the interfollicular epidermis is not established yet.

PAX3 and SOX10 are two transcription factors expressed in neural crest cells that are crucial for commitment to the melanocyte lineage. In adult human skin, PAX3 expression occurs in precursor cells and also in interfollicular melanocytes, with the exception of terminally differentiated melanocytes (*10, 13–15*). Similarly, SOX10 is expressed in undifferentiated and early-differentiated melanocytes, but then downregulated as the cells terminally differentiate (*16, 17*).

The role of PAX3 and SOX10 in the melanocyte lineage has been established in adult mice. Upon UVR exposure, PAX3 and SOX10 act synergistically in precursor cells to initiate melanocyte differentiation and melanin synthesis. Simultaneously, PAX3 prevents terminal differentiation, thereby rescuing a subset of precursor cells from depletion (*18, 19*). SOX10 also plays a role in the maintenance of this subset (*20*).

Microphthalmia-associated transcription factor (MITF) is expressed in neural crest cells downstream of PAX3 and SOX10. MITF is a nuclear protein critical for all stages of the melanocyte lineage (*21, 22*). However, to prevent melanocyte maturation, MITF expression is suppressed in quiescent melanocyte stem cells by TGF-β signaling from adjacent cells of the keratinocyte lineage in the hair follicle bulge (*11*). MITF regulates the major enzymes in melanin synthesis: tyrosinase, tyrosinase-related protein-1 and dopachrome tautomerase (DCT) (*23*). MITF also controls melanocyte proliferation and cell survival (*24*). Notably, PAX3 has been shown to govern the proliferation and survival of immature melanocytes through its role as a key regulator of MITF (*18, 19*). Simultaneously, MITF protects precursor melanocytes from premature differentiation via negative regulation of SOX10 (*20*). MITF is also critical for melanocyte survival via its regulation of the endogenous expression of the anti-apoptotic protein Bcl-2 (*25*).

Signaling through the secretion of cytokines by keratinocytes substantially regulates the survival of epidermal melanocytes, dendrite formation and melanin synthesis. For example, UVR-exposed melanocytes adjacent to keratinocytes have a superior survival rate to melanocytes without neighboring keratinocytes (*26*). In the case of unexposed human foreskin, constitutive TGF-β signaling from adjacent keratinocytes suppresses PAX3 in the precursor melanocytes, maintaining a quiescent, non-proliferating and non-melanin-producing state. Therefore, TGF-β regulates endogenous PAX3 expression in undifferentiated melanocytes in a paracrine dose-dependent manner (*8, 9*). UVR exposure represses paracrine TGF-β signaling from keratinocytes, subsequently upregulating PAX3 in immature melanocytes. The UVR sensors and effectors for skin pigmentation are mediated through the ATM/ATR/p53 and JNK pathways. Activation of both pathways upon UVR damage inhibits TGF-β secretion from keratinocytes by regulating activating-protein 1 (*9, 27*).

UVR induces phosphorylation and stabilization of the tumor repressor p53 in keratinocytes via ATM and ATR. Stabilized p53 in keratinocytes exerts at least three regulatory functions on melanocytes. First, p53 suppression of TGF-β secretion from keratinocytes results in upregulation of PAX3 in melanocytes. Second, p53 induces transcription of melanocyte-stimulating hormone (α-MSH), a ligand secreted to a much larger extent by keratinocytes than melanocytes, activating the melanocortin-1 receptor (MCIR) on melanocytes (*8, 9*). Alpha-MSH/MCIR induces the c-AMP pathway in melanocytes. SOX10 is upregulated, independent of p53, through UVR-induced inhibition of ATR function in melanocytes (*28*). Activation of the PAX3/c-AMP/SOX10 complex is necessary for initiating the transcription of MITF, and pushes immature melanocytes towards differentiation (*12, 19, 29*). A third regulatory function of stabilized p53 is that it induces stem cell factor (SCF) expression in keratinocytes. SCF is the ligand of the c-KIT receptor on melanocytes (*30*), and SCF/c-KIT signaling activates MITF (*31, 32*).

In human foreskin, proteins involved in the response of keratinocytes upon exposure to UVR, such as p53 and p38, also regulate the effects of UVR on melanocytes (*8, 9*). Similar findings have been reported in organ cultures of human skin (*30*) and hair follicles in mice (*33*). However, keratinocyte-melanocyte interactions upon exposure to

UVR have not yet been clarified in adult human interfollicular epidermis. Furthermore, it is unknown whether the paracrine cytokine signaling from keratinocytes to melanocytes, which manifests upon DNA damage from UVR, also occurs after exposure to ionizing radiation.

The goal of this study was to determine the response to low-dose fractionated irradiation of *in situ* epidermal interfollicular melanocytes, using UVR-related molecular markers.

MATERIALS AND METHODS

Patients and Radiotherapy

Skin biopsies were taken from 33 prostate cancer patients receiving radiotherapy with curative intent in Gothenburg, Sweden, between 2003 and 2005. The median age of the patients was 65 years (range 49–74 years). Approval was obtained from the Ethical Committee at the University of Gothenburg (Gothenburg, Sweden). Written informed consent was obtained from all patients prior to participation.

In accordance with ICRU50 (*34*), the prescribed radiation dose to the isocenter of the prostate was 35 daily fractions of 2 Gy for 7 weeks. Photons (11 or 15 MV) were applied in a three-field technique with one anterior field and opposed lateral fields with wedges. A 5-mm bolus was added on the left lateral field. The dose per fraction, at a depth of 0.1 mm below the skin surface (relevant for the biological end points), was determined carefully at the location where each biopsy was taken, as described in detail earlier (*3, 4*).

A total of 268 skin punch biopsies, 3 mm in diameter, were sampled. Four unexposed control biopsies (0 Gy) were collected from the hip region, not sun-exposed, for each patient prior to the start of the radiotherapy course and before the CT for dose planning and the simulation procedure. Four irradiated biopsies were taken during radiotherapy from each patient at the same occasion from skin areas that would correspond to doses of approximately 0.1, 0.2, 0.45 and 1.1 Gy, respectively. The two lowest dose per fractions were obtained by taking biopsies at 15 and 30 mm outside the lateral fields in the penumbra region. The two highest dose per fractions were obtained by taking biopsies within the lateral fields. The position of each sample in relationship to the treatment fields was transferred to a transparency film and was compared to the dose plan to further improve the dose determination for each of the four irradiated biopsies. The doses in the build-up region both inside and outside the treatment fields were determined by ionization chamber measurements in phantoms with a typical field set-up for these patients, as described in detail elsewhere (*3*). The estimated maximum uncertainty of the determined doses was less than 12% for the two lower doses and less than 7% for the two higher doses. The unique biopsy sampling procedure made it possible to determine dose-response relationships for each individual patient and all investigated end points for the cells of the melanocyte lineage.

The average and standard deviation of the individual dose estimations for each biopsy taken from the four different sites for all 33 patients were 0.05 ± 0.01, 0.13 ± 0.05, 0.44 ± 0.03 and 1.09 ± 0.08 Gy. Biopsies from the 33 patients were collected at two occasions during the radiotherapy course: group 1 (22 patients) at 1 week of radiotherapy and group 2 (12 patients) 6.5–7 weeks of radiotherapy. All biopsies were taken 30 min after the latest fraction and fixed immediately in 4% formaldehyde, dehydrated and embedded in paraffin.

Immunohistochemistry

Three transverse 4-μm tissue sections from each biopsy were taken from various levels and mounted on a Superfrost™ Plus Slide (Menzel-Gläser, Braunschweig, Germany). The slides were dried at 37°C overnight. Immunohistochemical staining was performed on a Ventana Benchmark® automated IHC stainer using the Ventana iView™ DAB detection kit (Ventana® Medical Systems, Tucson, AZ); subsequent manual counterstaining was performed with Meyers HTX. The primary antibodies were: monoclonal mouse antibody ΔNp63 (4A4) sc-8431, raised against amino acids 1-205 at the N-terminus of human ΔNp63 (1:200; Santa Cruz Biotechnology® Inc., Dallas, TX); monoclonal mouse antibody MITF clone D5 (1:50; Dako, Glostrup, Denmark); and monoclonal mouse antibody Bcl-2 clone 124 (1:15; Dako). In addition, three tissue sections from each biopsy were stained with hematoxylin and eosin (H&E) and periodic acid-Schiff (eosin-PAS). Tissues known to express the antigen of interest were used as positive controls. As negative controls, skin biopsy sections omitting the primary antibodies from the staining procedure were used. For each molecular marker, all tissue sections from one patient were stained simultaneously to avoid influence from fluctuations in the procedure.

Immunofluorescence

Combinations of primary antibodies from different species were used for double-staining: MITF (1:100, monoclonal mouse, clone D5; Dako), MITF (1:50, polyclonal rabbit; Atlas Antibodies, Bromma, Sweden), ΔNp63 (1:200, monoclonal mouse, clone 4A4; Santa Cruz Biotechnology), ΔNp63 (1:100, polyclonal rabbit; Atlas Antibodies), Bcl-2 (1:20, monoclonal mouse, clone 124; Dako), p53 (1:100, monoclonal mouse, clone DO-7; Dako), Ki-67 (1:100, monoclonal mouse, clone MIB-1; Dako), SOX10 (1:100, polyclonal goat, N-20; Santa Cruz Biotechnology), PAX3 (1:100, polyclonal rabbit; Invitrogen), p21 (1:100, monoclonal mouse, clone EA10; Abcam®, Cambridge, MA), c-KIT (1:100, polyclonal rabbit; Dako) and DCT (1:500, monoclonal mouse, clone C-9; Santa Cruz Biotechnology). Double-staining experiments were performed with appropriate pairs of fluorescent secondary antibodies raised in goat or donkey and attached to Alexa Fluor® 480 and 555 fluorescent dyes (1:100; Molecular Probes®, Eugene, OR). The manual staining protocol included epitope retrieval in boric acid buffer (pH 7.0) heated in a water bath (90°C) for 45 min. Antibody incubations were performed at 20°C for 1 h and followed by three 5-min washes in phosphate-buffered saline (pH 7.4). 4′,6-diamidino-2-phenylindole dilactate (DAPI, 0.4 μg/ml; Molecular Probes) was used for nuclear staining. Slides with air-dried sections were mounted in Vectashield® mounting media (Vector® Laboratories, Burlingame, CA).

Quantification of Molecular Markers

Quantitative estimates of melanocytes positive or negative for ΔNp63, MITF and/or Bcl-2 were determined by cell counting restricted to the basal layer of the epidermis. These cells can easily be distinguished from keratinocytes through the morphological characteristics revealed by eosin-PAS staining (*5, 6, 35*); melanocytes have distinct nucleoli, tendency for vacuolization, cytoplasm adherence to the nucleus and lack of desmosomes. ΔNp63 is a cell-cycle regulator expressed in keratinocytes but undetectable in normal melanocytes (*36*). The ΔNp63-negative cells fulfilled the morphological criteria of melanocytes. Therefore, all ΔNp63-negative cells were associated with the melanocyte lineage. The cell nucleus of the melanocyte very distinctly stains for MITF. In contrast, Bcl-2 protein is observed in the cytoplasm of melanocytes. However, Bcl-2 expression is undetectable in keratinocytes in the unexposed epidermis and also upon UVR exposure (*37*).

The total number of cells in the melanocyte lineage identified per mm of basal membrane was determined for all biopsies on three separate sections for eosin-PAS staining and each immunostaining. All counting was performed by one of the authors (P.F.) using a brightfield microscope with a 100× objective. The author I.H. also counted all eosin-PAS samples, with results equivalent to those of PF (linear regression, $R = 0.84$, $P < 0.001$, data not shown). With the use of 100× magnification the desmosomes of the keratinocyte cell membrane were clearly visualized in all immunohistochemical

TABLE 1
Mean Number of Cells per mm for each Marker and Patient Group

Staining	Group[a]	Dose per fraction				
		0 Gy	0.05 Gy	0.13 Gy	0.44 Gy	1.09 Gy
ΔNp63	1	17.4 (0.7)	18.9 (0.9)	19.2 (1.1)	18.7 (0.9)	18.7 (1.1)
	2	17.4 (1.3)	17.1 (1.2)	15.3 (0.8)	15.8 (1.4)	15.7 (1.4)
Eosin-PAS	1	18.7 (0.7)	21.7 (1.0)	22.1 (1.0)	22.1 (1.1)	23.6 (1.5)
	2	18.1 (1.3)	20.6 (1.3)	19.9 (1.2)	22.2 (1.4)	21.9 (1.4)
MITF positive	1	12.3 (0.7)	19.0 (1.2)	19.6 (1.2)	19.7 (1.1)	20.6 (1.2)
	2	13.5 (1.5)	16.0 (1.4)	17.1 (1.8)	20.1 (1.1)	21.6 (1.7)
MITF negative	1	5.5 (0.3)	4.1 (0.3)	3.1 (0.2)	2.6 (0.3)	1.8 (0.2)
	2	3.9 (0.4)	2.5 (0.3)	1.8 (0.2)	0.9 (0.2)	0.7 (0.1)
Bcl-2-positive	1	14.4 (0.7)	19.2 (1.2)	20.6 (1.2)	20.9 (0.9)	21.5 (1.3)
	2	15.3 (1.2)	18.8 (1.4)	19.4 (1.2)	21.8 (1.5)	22.5 (1.0)
Bcl-2-negative	1	4.6 (0.2)	2.9 (0.1)	2.07 (0.1)	1.5 (0.1)	1.2 (0.1)
	2	4.4 (0.2)	3.0 (0.3)	1.9 (0.2)	1.1 (0.1)	0.7 (0.1)

Note. Data are presented as mean (SE).
[a] Group 1: from patients after 1 week of radiotherapy (n = 22); group 2: from patients at the end (6.5–7 weeks) of radiotherapy (n = 12).

staining, facilitating the separation of melanocytes from keratinocytes located at the basement membrane.

To evaluate the presence of melanocyte-specific markers and DNA damage proteins expressed in melanocytes, ΔNp63 co-staining was assessed by immunofluorescence. We identified subpopulations positive or negative for each protein and co-expression of melanocyte-specific markers. An estimation of the number of cells within each subset of markers was intended.

Statistical Analysis

Repeated measures analysis of variance (ANOVA) was used for comparisons among the two patient groups. The correlation between dose and response for each individual was determined by Kendall's tau for each staining (*38*). The mean values of the individual correlation coefficients were tested in a one-sample *t* test with the hypothesis that the true mean equals zero. Statistical Package for the Social Sciences (SPSS version 22; Chicago, IL) and R were used for all statistical analyses (*39*).

Low-dose hypersensitivity was investigated by assessing the shapes of the individual dose-response curves for estimates of MITF- and Bcl-2-negative melanocytes. Individual dose-response relationships were normalized to dose fraction, providing a measure by which the effect per dose unit is comparable within each patient's biopsy set. The slopes from all individual regressions were collected and tested using a *t* test with the hypothesis that the true mean equals zero (*4*).

RESULTS

Table 1 shows the number of cells that expressed each marker at 1 week of radiotherapy (group 1, n = 22) and at 6.5–7 weeks of radiotherapy (group 2, n = 12).

ΔNp63 and Eosin-PAS Staining

All ΔNp63-negative cells fulfilled the morphological criteria for melanocytes (Fig. 1A). In unexposed skin, group 1 had 17.4 ± 0.7 ΔNp63-negative cells/mm. At 1 week of radiotherapy, the number of cells increased slightly, but not significantly, for all doses per fraction (Fig. 2A). In group 2, 17.4 ± 1.3 ΔNp63-negative cells/mm was estimated in unexposed skin; there was a small but insignificant decrease in the number of ΔNp63-negative cells for all doses per fraction at 6.5 weeks of radiotherapy. Overall, no significant difference was found in the number of ΔNp63-negative cells at 1 week and 6.5 weeks of radiotherapy (Table 1). We conclude that, independent of dose per fraction, no significant loss of cells in the melanocyte lineage occurred during the radiation treatment.

In contrast to keratinocytes in eosin-PAS-stained skin sections, melanocytes lacked desmosomes and had a halo around the cell, making them easy to identify in the basal layer of the epidermis. Notably, after exposure to a small radiation dose, the halo became more prominent (Fig. 1B). In group 1, 18.7 ± 0.7 melanocytes/mm were estimated in unexposed skin. At 1 week of radiotherapy, the number of cells increased slightly up to 23.6 ± 1.5 cells/mm over the dose range 0.05–1.08 Gy ($P < 0.001$) (Fig. 2B). In group 2, the number of melanocytes in unexposed skin was 18.1 ± 1.3 cells/mm. This number increased at 6.5 weeks of radiotherapy, up to 21.9 ± 1.4 over the dose range 0.05–1.11 Gy, but was only significant for 0.44 Gy. However, no significant difference was found between 1 and 6.5 weeks of radiotherapy at any dose (Table 1).

The accuracy of identifying interfollicular melanocytes was supported by the correlation between the number of ΔNp63-negative cells and eosin-PAS for individual patients. We found a strong correlation between eosin-PAS-determined melanocytes and ΔNp63-negative cells in both unexposed skin ($P < 0.001$; Fig. 3A) and irradiated skin ($P < 0.001$; Fig. 3B).

Immunohistochemical Staining of MITF and Bcl-2

After 1 week of radiotherapy, a gradual increase in the number of MITF-positive marker MITF appeared in the nucleus (Fig. 1C). Group 1 had 12.3 ± 0.7 MITF-positive cells/mm in unexposed skin. A gradual increase up to 20.6

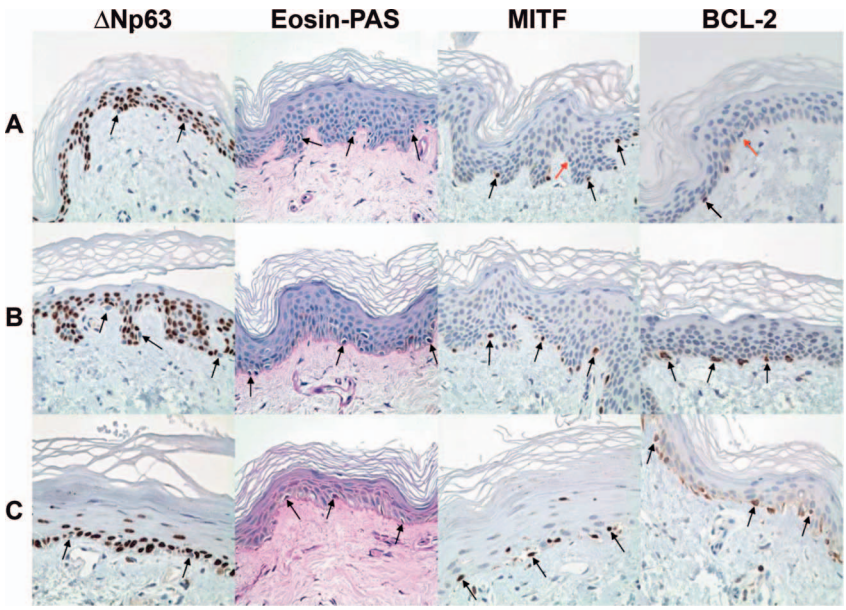

FIG. 1. Immunohistochemistry for ΔNp63, eosin-PAS, MITF and Bcl-2 in skin biopsies. Row A: Before radiotherapy. Row B: One week of radiotherapy. Row C: Six and half weeks of radiotherapy. In the MITF staining, black arrows indicate examples of MITF-positive melanocytes and red arrows indicate MITF-negative melanocytes.

± 1.2 cells/mm was observed over the dose range 0.05–1.08 Gy ($P < 0.001$) (Fig. 2C). In group 2, the number of MITF-positive cells was estimated to be 13.5 ± 1.5 cells/mm in unexposed skin, gradually increasing to 21.6 ± 1.7 cells/mm at the end of radiotherapy over the dose range 0.05–1.11 Gy ($P < 0.001$). No significant difference was found between 1 and 6.5 weeks of radiotherapy at any dose per fraction (Table 1).

All MITF-positive cells in the basal layer possessed the morphological features of melanocytes. Some cells that were identified as melanocytes did not stain for MITF. In particular, their specific location at the basement membrane and lack of desmosomes unequivocally distinguished them from adjacent keratinocytes. We refer to these cells as MITF-negative melanocytes (Table 1, Fig. 1C). In group 1, the number of MITF-negative melanocytes was 5.5 ± 0.3 cells/mm in unexposed skin. At 1 week of radiotherapy, there was a significant gradual decrease in the number of MITF-negative melanocytes, down to 1.8 ± 0.2 cells/mm over the dose range 0.05–1.08 Gy ($P < 0.001$) (Fig. 2C). In group 2, the number of MITF-negative melanocytes was 3.9 ± 0.4 cells/mm in unexposed skin. At 6.5 weeks of radiotherapy, a significant gradual decrease in the number of MITF-negative melanocytes was measured, down to 0.7 ± 0.1 cells/mm over the dose range 0.05–1.11 Gy ($P < 0.001$, Table 1). The dose response at 1 week of radiotherapy did not significantly differ from the dose response at 6.5 weeks of radiotherapy. The dose-dependent reduction in the number of MITF-negative melanocytes demonstrated a low-dose hypersensitive response at both 1 and 6.5 weeks of radiotherapy and was detected for each patient ($P < 0.001$).

Bcl-2 staining was restricted to melanocytes in the basal cell layer (Fig. 1D). All Bcl-2-positive cells exhibited the morphological characteristics of melanocytes. In group 1, the number of Bcl-2-positive cells in unexposed skin was estimated to be 14.4 ± 0.7 cells/mm. At 1 week of radiotherapy, there was a gradual increase in the number of Bcl-2-positive cells, up to 21.5 ± 1.3 cells/mm over the dose range 0.05–1.08 Gy ($P < 0.001$) (Fig. 2D). In group 2, the number of Bcl-2-positive cells was 15.3 ± 1.2 cells/mm in unexposed skin. After 6.5 weeks of radiotherapy, the number gradually increased to 22.5 ± 1.0 cells/mm over the dose range 0.05–1.11 Gy ($P < 0.001$, Table 1). No significant difference in dose response was found between 1 and 6.5 weeks of radiotherapy.

In parallel to the existence of MITF-negative cells, some cells identified as melanocytes did not stain for Bcl-2. We refer to these cells as Bcl-2-negative melanocytes (Fig. 1D). In group 1, the number of Bcl-2-negative melanocytes was 4.6 ± 0.2 cells/mm in unexposed skin. At 1 week of radiotherapy, there was a significant gradual decrease in the number of Bcl-2-negative melanocytes, down to 1.2 ± 0.09 cells/mm over the dose range 0.05–1.08 Gy ($P < 0.001$) (Fig. 2D). In group 2, the number of Bcl-2-negative melanocytes was 4.4 ± 0.2 cells/mm in unexposed skin. At 6.5 weeks of radiotherapy, a significant gradual decrease in the number of Bcl-2-negative melanocytes, down to 0.7 ± 0.1 cells/mm, was recorded over the dose range 0.05–1.11 Gy ($P < 0.001$, Table 1). The dose response at 1 week of radiotherapy did not significantly differ from the dose

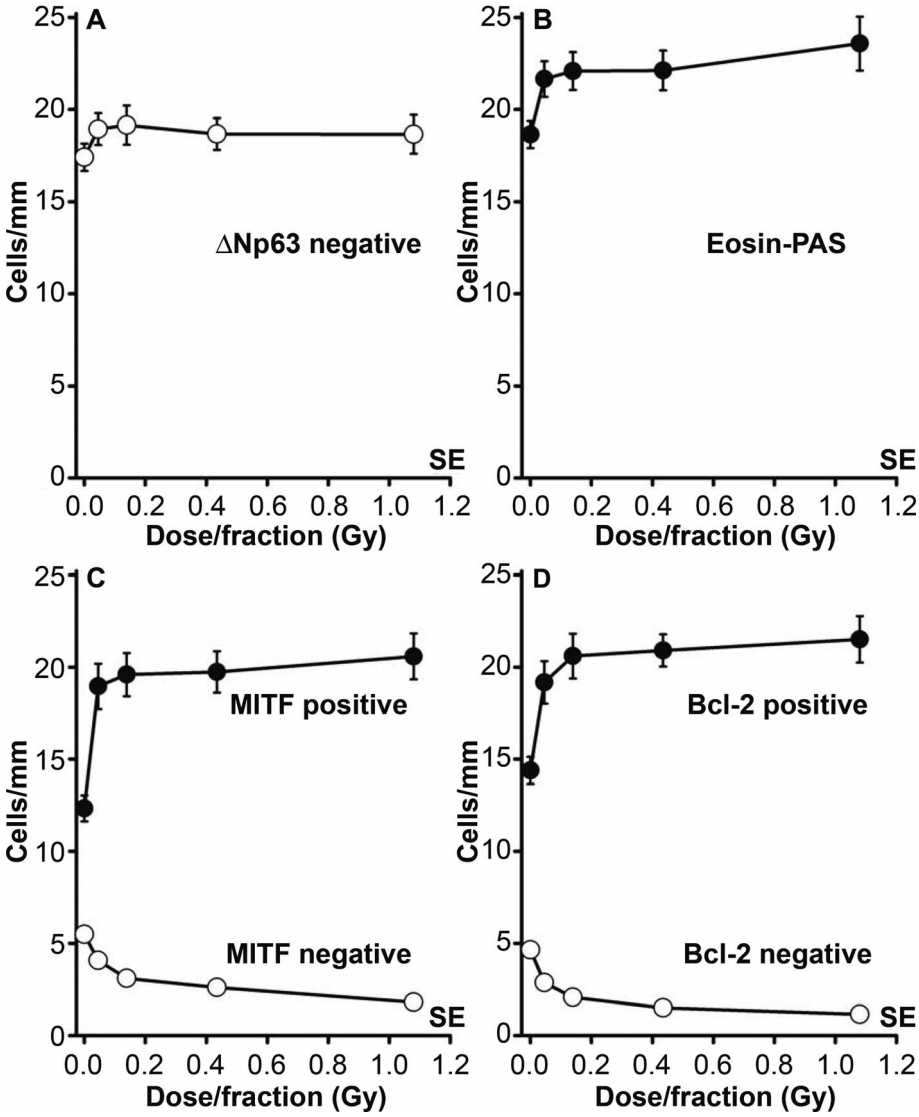

FIG. 2. Mean number of stained cells per mm in the basal layer for various molecular markers at 1 week of radiotherapy. Panel A: ΔNp63-negative cells. Panel B: Morphological characterization via eosin-PAS staining. Panel C: MITF-positive cells and MITF-negative cells morphologically characterized as melanocytes. Panel D: Bcl-2-positive cells and Bcl-2-negative cells morphologically characterized as melanocytes. Error bars represent standard error. Error bars for MITF and Bcl-2-negative cells are hidden within the symbols.

response at 6.5 weeks of radiotherapy. The dose-dependent reduction in Bcl-2-negative cells demonstrated a low-dose hypersensitive response at both 1 and 6.5 weeks and was detected for each patient ($P < 0.001$).

There was good agreement regarding the number of MITF-positive and Bcl-2-positive cells, and MITF-negative and Bcl-2-negative cells in unexposed and irradiated skin (Table 1, Fig. 2C and D). Importantly, we also demonstrated high correlation between MITF and Bcl-2-positive cells for the individual patient in both unexposed and irradiated skin at all four dose levels (Fig. 4).

Immunofluorescent Staining for MITF and Bcl-2

To confirm that all MITF- and Bcl-2-positive and negative cells identified by immunohistochemical staining belong to the melanocyte lineage, we co-stained each MITF and Bcl-2 with ΔNp63 (Fig. 5A and B). No ΔNp63-positive cell in unexposed or irradiated skin co-expressed MITF or Bcl-2. In unexposed skin, a subset of ΔNp63-negative cells was also negative for MITF and Bcl-2. After exposure with the largest dose per fractions (1.1 Gy), at the very most one or two MITF-negative and Bcl-2-negative melanocytic cells/mm were detected. Thus, a true reduction in the subsets of MITF- and Bcl-2-negative melanocytes was observed after irradiation. Co-staining for MITF and Bcl-2 indicated complete overlap in the expression of the two proteins; no cells stained exclusively for MITF or Bcl-2 (Fig. 5C).

Taken together, the assessments made by double-staining for ΔNp63 were consistent with the morphological

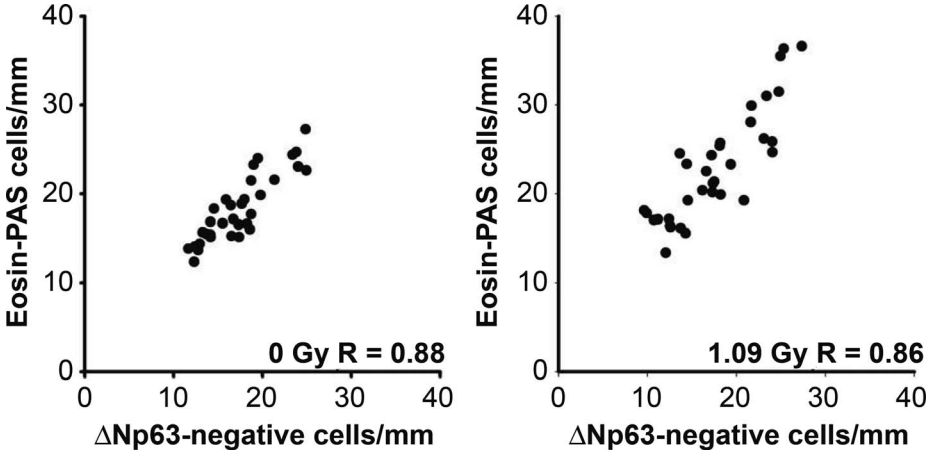

FIG. 3. The number of eosin-PAS-determined melanocytes and ΔNp63-negative cells for all 33 individual patients. Panel A: Unexposed skin. Panel B: Irradiated skin, 1.09 Gy per fraction. The correlations are significant ($P < 0.001$).

identification of negatively and positively stained melanocytes via immunohistochemistry for both MITF and Bcl-2. Importantly, we identified a subset of MITF-negative and Bcl-2 negative melanocytes, i.e., undifferentiated melanocytes, which demonstrate dose-dependent disappearance upon exposure to ionizing radiation. Furthermore, the reduction in negative cells was associated with a corresponding increase in cells positive for the two proteins. Notably, we verified that the upregulation of Bcl-2 parallels the upregulation of MITF (Table 1, Figs. 2C and D, and 4).

Immunofluorescent Staining for MITF, SOX10 and PAX3

Co-staining for SOX10 and ΔNp63 revealed SOX10-positive cells exclusively among the ΔNp63-negative cells. In unexposed skin, approximately 25% of the ΔNp63-negative cells were SOX10-positive, and the number increased substantially, to at least 50%, after irradiation (data not shown). The results of double-staining for MITF and SOX10 are shown in Fig. 5D. In unexposed skin, we noted the presence of cells co-staining for both markers or only for SOX10 or MITF. In the irradiated samples, the number of double-stained cells increased. Thus, ionizing radiation induced an increase in SOX10 expression and increased MITF activity in cells that also expressed SOX10.

Co-staining for PAX3 and ΔNp63 revealed that PAX3-positive cells were found exclusively in the ΔNp63-negative cell population, in both unexposed and irradiated skin (Fig. 5E). In unexposed skin, approximately one third of ΔNp63-negative cells were PAX3-negative, and at 1 week of radiotherapy (1.1 Gy) the majority were PAX3-positive.

In unexposed skin, double-staining for PAX3 and MITF revealed PAX3-positive/MITF-negative cells, PAX3-negative/MITF-positive cells and cells expressing both proteins. At 1 week of radiotherapy, the majority of stained cells expressed both proteins; only a few cells stained for MITF alone after 1.1 Gy per fractions (Fig. 5F).

Double-staining unexposed skin for PAX3 and SOX10 revealed PAX3-negative/SOX10-positive cells, PAX3-positive/SOX10-negative cells, and cells expressing both proteins in approximately one third of each part. At 1 week of radiation treatment with 1.1 Gy per fraction the majority of cells expressed both proteins, confirming the induction of both PAX3 and SOX10 upon ionizing radiation exposure (Fig. 5G).

Immunofluorescent Staining for Proliferation

To determine whether proliferation of cells in the melanocyte lineage occurred throughout the irradiation period, we co-stained for Ki-67 and ΔNp63 (Fig. 5H). As previously shown by immunohistochemistry, an increasing proportion of epidermal keratinocytes expressed Ki-67 throughout the 7 weeks of radiation treatment (*40*). In contrast, all cells in the melanocyte lineage (ΔNp63-negative cells) were negative for Ki-67. Thus, proliferation is not indicated in the melanocyte population over 7 weeks of radiation treatment and proliferation cannot explain the significant increase in the number of MITF-positive and Bcl-2 positive cells upon ionizing radiation exposure described above.

Immunofluorescent Staining of p53 and p21

We double-stained p53 and ΔNp63 to reveal any upregulation of p53 (Fig. 5I). The expression of p53 in epidermal keratinocytes was previously shown by immunohistochemistry to increase throughout radiation treatment (*40*), which was also obvious in the current double-staining. However, all ΔNp63-negative cells were also negative for p53. Thus, the melanocyte population did not express p53 upon ionizing radiation exposure.

Upregulation of p53 in keratinocytes is associated with the transcription of p21. The results of co-staining for p21 and ΔNp63 are shown in Fig. 5J. In agreement with the lack of p53 expression in melanocytes, no nuclear p21 staining

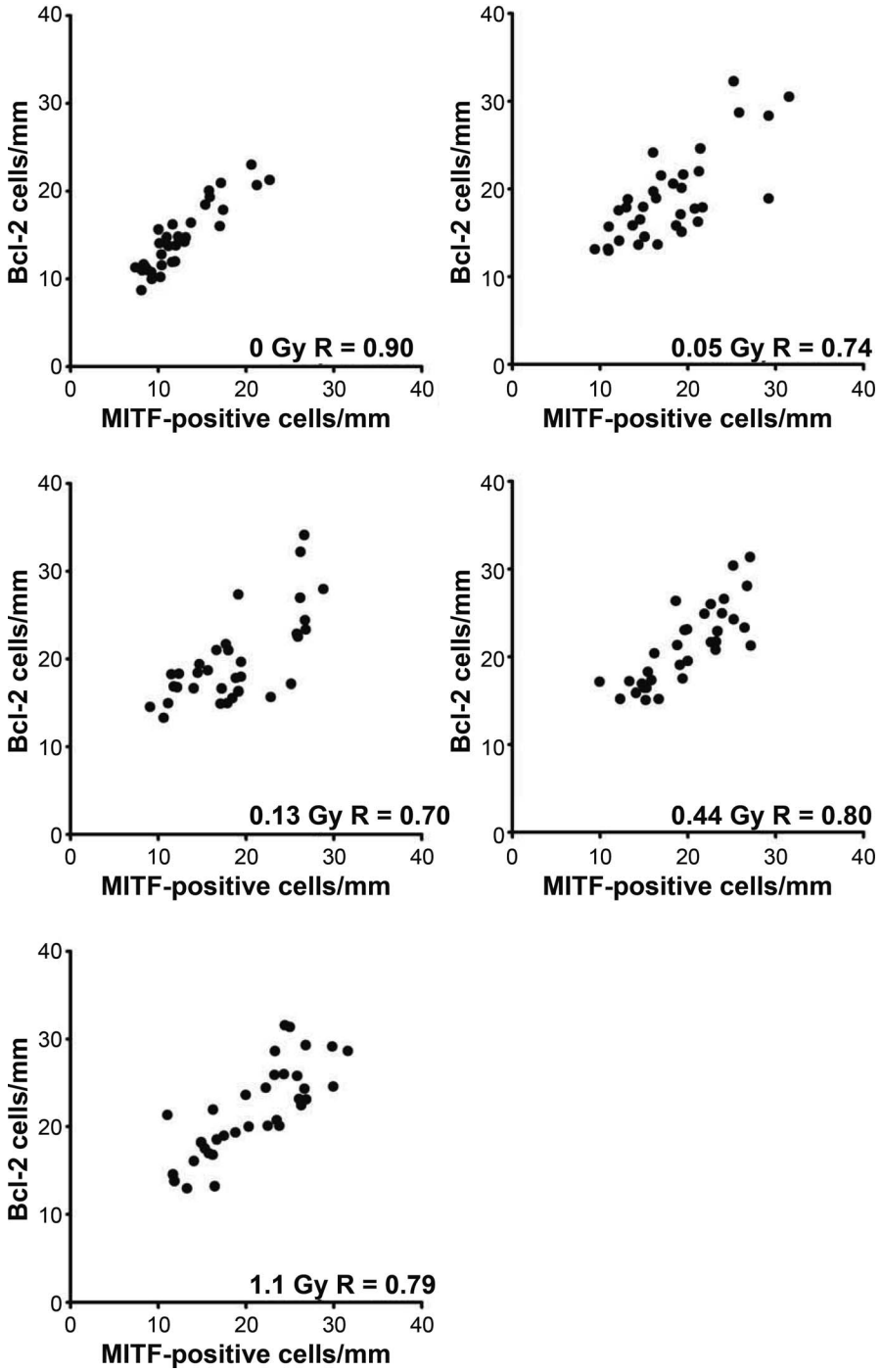

FIG. 4. The number of Bcl-2-positive vs. MITF-positive cells for all 33 individual patients in unexposed control samples and for each dose of fractionated radiation. The correlations are significant ($P < 0.001$).

was detected in ΔNp63-negative cells, though we did observe weak staining in the cytoplasm. However, upregulation of p21 was evident in keratinocytes as shown in previously published studies (*4, 40*).

Activation of c-KIT and DCT

Co-staining for c-KIT and ΔNp63 revealed that c-KIT-positive cells were found exclusively among the ΔNp63-negative cells. Approximately one half of the cells in unexposed skin were c-KIT-positive, and the number increased gradually at 1 and 6.5 weeks of radiotherapy (Fig. 5K). Double-staining for c-KIT and MITF showed that in unexposed skin, all MITF-positive cells were c-KIT-positive and all MITF-negative cells were also c-Kit-negative (data not shown).

Double-staining for DCT and ΔNp63 showed that approximately one half of the ΔNp63-negative cells in

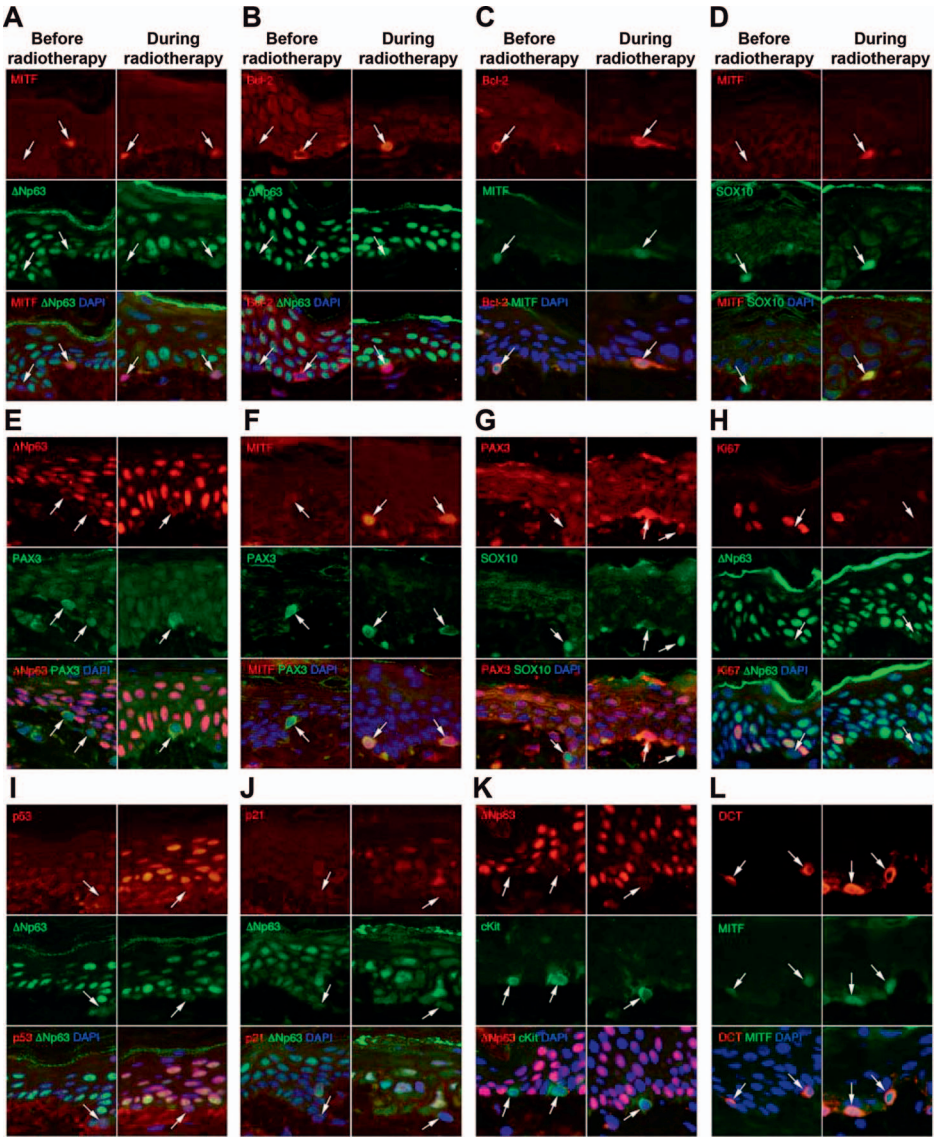

FIG. 5. Double-staining of epidermal skin biopsies illustrating the response of melanocytes to daily fractionated treatments of 1.1 Gy. Cells in the melanocyte lineage are exclusively negative for ΔNp63. Each double-staining was merged with DAPI. Panel A: Double-staining for ΔNp63 and MITF. Before radiotherapy, the left arrows indicate an MITF-negative melanocyte and right arrows indicate a MITF-positive melanocyte in the basal layer. During radiotherapy, the arrows indicate MITF-positive melanocytes. Panel B: Double-staining for ΔNp63 and Bcl-2. Before radiotherapy, the left arrows indicate a Bcl-2-negative melanocyte and right arrows indicate a Bcl-2-positive melanocyte in the basal layer. During radiotherapy, the arrows indicate a Bcl-2-positive melanocyte. Panel C: Double-staining for MITF and Bcl-2. Arrows indicate Bcl-2 cells co-expressing MITF and vice versa before and during radiotherapy. Panel D: Double-staining for MITF and SOX10. Before radiotherapy, the left arrows indicate a MITF-negative/SOX10-positive melanocyte in unexposed skin. During radiotherapy, the arrows indicate a MITF-positive/SOX10-positive melanocyte. Panel E: Double-staining for ΔNp63 and PAX3. The arrows indicate ΔNp63-negative/PAX3-positive melanocytes before and during radiotherapy. Panel F: Double-staining for MITF and PAX3. Before radiotherapy, the arrows indicate a MITF-negative/PAX3-positive melanocyte. During radiotherapy, the arrows indicate melanocytes that co-express MITF and PAX3. Panel G: Double-staining for PAX3 and SOX10. Before radiotherapy, the arrows indicate a PAX3-negative/SOX10-positive melanocyte. During radiotherapy, the left arrows indicate a PAX3-positive/SOX10-negative melanocyte and right arrows indicate a PAX3-negative/SOX10-positive melanocyte. Panel H: Double-staining for ΔNp63 and Ki-67. The arrows indicate Ki67-negative/ΔNp63-negative melanocytes before and during radiotherapy. Panel I: Double-staining for ΔNp63 and p53. The arrows indicate p53-negative/ΔNp63-negative melanocytes before and during radiotherapy. Panel J: Double-staining for p21 and ΔNp63. The arrows indicate nuclear p21-negative/ΔNp63-negative melanocytes before and during radiotherapy. Panel K: Double-staining for c-KIT and ΔNp63. The arrows indicate ΔNp63-negative/c-KIT-positive melanocytes before and during radiotherapy. Panel L: Double-staining for DCT and MITF. The arrows indicate DCT-positive/MITF-positive melanocytes before and during radiotherapy.

unexposed skin were DCT-positive. The number of DCT-positive cells increased gradually with 1 and 6.5 weeks of radiation treatment. After 6.5 weeks, almost all ΔNp63-negative cells were DCT-positive (data not shown). Furthermore, DCT double-stained with MITF confirmed an increase in the number of MITF-positive/DCT-positive cells over the course of radiation treatment. At the end of treatment, almost all cells were stained for MITF and DCT. In unexposed skin, MITF-negative cells were DCT-negative, but MITF-positive cells also expressed DCT to some extent (Fig. 5L). After exposure, the melanocytes expressed higher levels of DCT and increase in the number of dendrites.

DISCUSSION

Quantification of Melanocytes by ΔNp63 and Eosin-PAS Staining

ΔNp63, an isoform of p63, is a key lineage-specific determinant of stratified epithelia, such as that of the epidermis (*41–44*). ΔNp63 is the predominant p63 isoform identified to date. Although total p63 is minimally expressed in normal melanocytes (*45*), melanocytes express small amounts of two of the six isoforms of p63, which have not been definitively determined. Importantly, none of the p63 isoforms are induced by ionizing radiation or UVR (*36*). We used the 4A4 anti-p63 monoclonal antibody in a manner similar to other studies and found intense staining of keratinocytes in the basal and suprabasal cell layers (Fig. 1A). The ΔNp63 staining was of variable intensity in keratinocytes (Figs. 1A, 5A, 5B, 5H–K) and comparable to previously reported findings (*41*). In light of the intense p63 staining, we cannot exclude the possibility that a small amount of p63 expression in melanocytes may serve as a confounding factor leading to a slight underestimation of the number of melanocytes (Table 1, Fig. 2A). By using decreasing concentrations of the 4A4 anti-p63 monoclonal antibody (from 1:100 up to 1:4,000), we found that 1:800 would have been the most optimal concentration, giving a 10% higher number of ΔNp63-negative cells than the 1:200 concentration used in this study (data not shown).

MITF-mediated activation of melanin-synthesizing enzymes requires the chromatin remodeling SWI/SNF complexes (*46*), which are necessary for MITF-based regulation of melanocyte differentiation. MITF recruits SWI/SNF complexes to the promoters of melanocyte-specific genes responsible for melanin synthesis, where the SWI/SNF enzymes remodel the chromatin to activate gene expression. Chromatin remodeling by the SWI/SNF complexes may induce the morphological changes in cells of the melanocyte lineage that were observed by eosin-PAS staining after low-dose irradiation (Fig. 1). Undifferentiated cells in unexposed skin are not visualized as easily by eosin-PAS staining as those in irradiated skin, which may lead to an underestimation of their number in control biopsies. This scenario is the most likely explanation for the significant increase in melanocytes after irradiation in the morphological evaluation (Table 1 and Fig. 2B).

Despite the confounding factors considered for the current ΔNp63 and eosin-PAS staining, the accuracy of the determined numbers of interfollicular melanocytes is satisfactory due to the strong correlation between the two estimations for individual patients in both unexposed and irradiated skin (Fig. 3).

Individual Variability in Melanocyte Density Assessed by Various Molecular Markers

Very little is found in the literature that addresses the density of cutaneous melanocytes. Barlow *et al*. determined the density of epidermal melanocytes by H&E staining of 6-μm sections; at 40× magnification the mean ± SD number of cells was 7.96 ± 6.7 cells/mm (*35*). No difference in melanocyte density was found between skin samples taken from regions of the head, neck, trunk and extremities. Furthermore, no difference in melanocyte density was found between skin types. Barlow *et al*. also reported a high degree of individual variability in melanocyte density, ranging from 0.7 to 33.4 cells/mm of epidermis [coefficient of variation (CV) 84%]. Tadokoro *et al*. (*47*) determined the melanocyte density in the basal layer to be 12.8 ± 1.2 melanocytes/mm by counting cells positive for MITF, MART-1, Pmel17 and tyrosinase. Shin *et al*. (*17*) reported 19.6 ± 5.7 cells/mm for the MITF-positive melanocyte density in normal skin. In these studies, no particular considerations were mentioned regarding the history of sun exposure for the investigated skin.

In the current study, the interfollicular epidermal melanocyte density was determined comprehensively. In unexposed skin, we counted 17.4 and 18.4 melanocytes/mm of epidermis for ΔNp63-negative cells and morphologically assessed melanocytes (eosin-PAS staining), respectively. The corresponding ranges in patients were 12–24 cells/mm for ΔNp63 staining and 12–27 cells/mm for eosin-PAS staining; the CVs were 22% and 20%, respectively.

The maximum number of melanocytes determined in the MITF and Bcl-2 staining experiments after irradiation were 20.9 and 21.9 cells/mm, respectively. The CV for MITF number was 27% and for the Bcl-2 number 23%. The individual variability in melanocyte density, though rather limited in our assessment, was confirmed by the strong correlation between Bcl-2-positive and MITF-positive melanocytes in unexposed skin and irradiated skin (Fig. 4). Collectively, individual variability in melanocyte density was threefold lower in our study than reported by Barlow *et al*. (*35*).

In the patient cohort presented here, the number of basal keratinocytes was determined to be 160 cells/mm (*4*). Based on all staining experiments, the number of melanocytes was 18–23 cells/mm, indicating that cells in

the melanocyte lineage comprise close to 13% of the cells in the basal cell layer of the interfollicular epidermis. These data are associated with a Swedish male population usually presenting with skin types 2 and 3; skin types 1 and 4 are rare in this population (*48, 49*). Furthermore, the assessments were performed using skin biopsies taken from the hip region, which is not usually exposed to sun. No significant correlation between patient age and melanocyte density was found in the range of 49 to 74 years.

Quantification of MITF and Bcl-2

The number of MITF-positive cells gradually increased with daily dose per fraction of 0.05–1.09 Gy when assessed at 1 and 6.5 weeks of radiotherapy, with similar dose responses at the two time points (Table 1). The number of MITF-negative melanocytes decreased in a dose-dependent manner within the same dose range and exhibited hyper-radiosensitivity to fractionated doses as low as 0.05 Gy (Table 1). The decrease in MITF-negative cells with dose precisely reflects the increase in MITF-positive melanocytes and indicates hypersensitivity to differentiation at doses below 0.3 Gy (Fig. 2C). Co-staining for ΔNp63 and MITF demonstrated the existence of MITF-negative cells, i.e., undifferentiated melanocytes, in the interfollicular melanocyte population and their disappearance after irradiation (Fig. 5A).

Similarly, the number of Bcl-2-positive melanocytes increased gradually with daily dose per fraction of 0.05–1.09 Gy, with a similar dose response at 1 and 6.5 weeks of radiotherapy (Table 1). In addition, the number of BCL-2-negative melanocytes decreased and hyperradiosensitivity was demonstrated at doses below 0.3 Gy (Fig. 2D). The connection between MITF and Bcl-2 is expected from *in vitro* studies showing that MITF promotes cell viability by regulating Bcl-2 (*25*). Here, we confirmed that this regulation persists in the clinical setting of radiotherapy, as illustrated by the strong correlation between Bcl-2 and MITF levels in each patient (Fig. 4). This observation was confirmed by the one-to-one correspondence in MITF and Bcl-2 co-staining (Fig. 5C).

Apoptosis and Proliferation

Melanocyte resistance to genotoxic stress has been attributed to upregulation of anti-apoptotic protein Bcl-2 by MITF (*25*). In addition, melanocytes have been confirmed to be resistant to UVR-induced apoptosis mediated by the activation of MITF in association with SWI/SNF complexes (*46, 50*). Importantly, the SWI/SNF complexes prevent DNA damage-induced apoptosis, an effect that is related, at least in part, to the ability of SWI/SNF complexes to repair DNA DSBs (*51*). Thus, the SWI/SNF complexes exert strong effects on the fate of melanocytes by driving differentiation and preventing apoptosis after genotoxic insult.

In a previously reported evaluation of apoptosis in the basal cell layer, only 0.2–1.5 apoptotic cells/mm was detected in the patient groups; the highest rate was observed after receiving 1.1 Gy dose fractions for 6.5 weeks (*4*). Therefore, we conclude that apoptosis in the epidermal melanocyte population is negligible. Notably, in a numerical comparison, cell death by apoptosis cannot explain the disappearance of MITF- and Bcl-2-negative cells upon exposure to ionizing radiation.

Ki-67 staining allowed us to exclude the possibility of significant melanocyte proliferation during the 7 weeks of treatment, supporting the consistent number of ΔNp63-negative cells observed during treatment (Fig. 2A). We can also state that the increase in MITF- and Bcl-2-positive cells upon ionizing radiation exposure is not caused by proliferation.

Differentiation Status of Skin Melanocytes

In this study we conclusively show that a subset of interfollicular melanocytes in unexposed skin is MITF-negative; these were also DCT-negative and c-KIT-negative. In this subset, we identified PAX3-positive and SOX10-positive cells. To the best of our knowledge, this finding is unique. We believe that the main reason that we could reveal a subset of MITF-negative melanocytes is that all biopsies were taken from the hip region, which is not usually exposed to sun. Furthermore, we established dose-response relationships showing how the number of MITF-negative cells decrease and the number of MITF-positive cells increase after exposure for each individual patient. This finding suggests a prompt need to further characterize the subset of MITF-negative cells among interfollicular melanocytes; in particular, if melanocyte stem cells do exist or if the undifferentiated cells are transit amplifying cells migrated from the hair bulge.

In the hair follicular bulge area of human skin the melanocyte stem cells are $DCT^{+}c\text{-}KIT^{-}$ and the melanoblasts are $DCT^{+}c\text{-}KIT^{+}$, but $DCT^{-}c\text{-}KIT^{+}$ cells have also been identified. Subsets of melanocyte precursor cells in the bulge area are PAX3-positive and SOX10-positive. MITF expression occurs only transiently (*10, 12*). In the interfollicular epidermis, subsets of cells express DCT, c-KIT, PAX3, SOX10 and MITF. Co-expression of the various markers is not well known. However, a variable differentiation status among interfollicular melanocytes were identified by Medic and Ziman (*15*), showing that approximately 20% of the melanocytes were less differentiated.

Radioresistance Induced by Differentiation

In the current study, we established that melanocytes are radioresistant regarding cell death and remain constant in number to fractionated doses below 1.1 Gy over the 7 weeks of treatment. The upregulation of MITF induced by UVR requires activation of PAX3, SOX10 and c-AMP. UVR-

induced c-KIT activity also promotes MITF expression. We established that increased expression of both PAX3 and SOX10 occurs in parallel with upregulation of MITF after irradiation and also observed an increase in c-KIT. Further evidence of differentiation after irradiation was established by staining for DCT, which revealed increased numbers of DCT-positive cells, enhanced staining intensity and higher density of enlarged dendrites after irradiation (Fig. 5L). Taken together, the first steps of radiation-induced melanin synthesis were confirmed.

The double-staining experiments with SOX10 and MITF, PAX3 and MITF, SOX10 and PAX3, and MITF and DCT that were used in our current study suggest similar regulation of MITF transcription after irradiation and what has already been established for UVR exposure, with the initiation of differentiation as the major response mechanism (Fig. 5D, F and G).

In support of our findings, differentiation as a response to ionizing radiation was confirmed for melanocyte stem cells in the hair follicle bulge of adult mice (*29*). After 5 Gy irradiation, melanocyte stem cells lose their immaturity and renewal to become melanin-producing dendritic melanocytes.

Keratinocyte-Melanocyte Interactions

Upon exposure to ionizing radiation, nuclear expression of p53 and p21 was very weak and considered negative in melanocytes compared to surrounding keratinocytes (Fig. 5I and J). This phenomenon was reported previously for human skin after exposure to UVR (*52, 53*), but the molecular pathways that suppress the p53-p21 pathway in melanocytes is poorly understood. However, PAX3 was recently shown to inactivate the function of p53 by stimulating its ubiquitination and degradation (*54*). Furthermore, ATR function is suppressed in melanocytes after UVR exposure and chemotherapy (cisplatin), suggesting a lack of activation of p53 and, subsequently, p21 (*28*). This particular response in melanocytes is also expected after radiation-induced DNA damage. Interestingly, ATR inhibition was confirmed to protect noncycling human cells exposed to UVR from undergoing apoptosis (*55*). Specific regulation of ATM kinase in melanocytes is still not known.

In a previously published study, although p21 mRNA and protein levels increased after DNA damage to melanocytes, p53 binding to p21 promoter DNA was undetectable (*36*). The lack of p53 and p21 expression in melanocytes in the current study highlights the critical role of ionizing radiation-induced p53 expression in keratinocytes and its associated paracrine signaling to melanocytes. The dose-dependent ATM-driven paracrine signaling from keratinocytes is reflected in the hypersensitive dose-dependent increase in MITF expression by melanocytes in parallel with the hypersensitivity found for all end points studied in keratinocytes (*4*).

We suggest that the hypersensitivity response toward melanocyte differentiation reflects incomplete phosphorylation of ATM in keratinocytes over the low-dose range (*56*) and corresponding incomplete dose-dependent paracrine signaling from keratinocytes. It has been previously established that skin keratinocytes exhibit hypersensitivity below 0.3 Gy for DNA DSBs, growth arrest, mitosis, apoptosis and overall cell loss (*2–4*).

In conclusion, constant levels of ΔNp63-negative cells suggest that the number of cells in the melanocyte lineage is preserved throughout the fractionated radiation therapy over 6.5 weeks at doses up to 1.1 Gy. A subpopulation of undifferentiated MITF- and Bcl-2-negative cells exists in unexposed interfollicular epidermis. After exposure to low doses of ionizing radiation, this subset of cells upregulates MITF and Bcl-2 in association with increased expression of PAX3, SOX10, c-KIT and DCT, indicating that differentiation and radioresistance for cell death is induced. The results suggest that the initial steps of melanin synthesis are common after exposure to ionizing radiation and UVR.

ACKNOWLEDGMENTS

We finalized this work thanks to long-term funding from the Swedish Cancer Society, the Research Foundation of the Department of Oncology at the University of Uppsala, the Lions Cancer Research Foundation in Uppsala and the King Gustav V Jubilee Clinic Cancer Research Foundation in Gothenburg. Financial support was also received from Uppsala University Hospital and from the Centre for Research and Development, Uppsala University/Region Gävleborg, Sweden. We thank Karl-Axel Johansson for meticulous dosimetry and Majlis Book for help with histological work and skillful accomplishment of immunohistochemistry. We are grateful to Hans Högberg and Per Liv for statistical support. We also very much appreciate Jolyon Hendry for comments on the manuscript.

Received: March 7, 2018; accepted: October 11, 2018; published online: November 8, 2018

REFERENCES

1. Joiner MC, Marples B, Lambin P, Short SC, Turesson I. Low-dose hypersensitivity: current status and possible mechanisms. Int J Radiat Oncol Biol Phys 2001; 49:379–89.
2. Qvarnstrom F, Simonsson M, Nyman J, Hermansson I, Book M, Johansson KA, et al. Double strand break induction and kinetics indicate preserved hypersensitivity in keratinocytes to subtherapeutic doses for 7 weeks of radiotherapy. Radiother Oncol 2017; 122:163–69.
3. Simonsson M, Qvarnstrom F, Nyman J, Johansson KA, Garmo H, Turesson I. Low-dose hypersensitive gammaH2AX response and infrequent apoptosis in epidermis from radiotherapy patients. Radiother Oncol 2008; 88:388–97.
4. Turesson I, Nyman J, Qvarnstrom F, Simonsson M, Book M, Hermansson I, et al. A low-dose hypersensitive keratinocyte loss in response to fractionated radiotherapy is associated with growth arrest and apoptosis. Radiother Oncol 2010; 94:90–101.
5. Fitzpatrick TB, Wolff K. Fitzpatrick's dermatology in general medicine. 7th ed. New York: McGraw-Hill Medical; 2008.
6. Lin JY, Fisher DE. Melanocyte biology and skin pigmentation. Nature 2007; 445:843–50.
7. Park HY, Kosmadaki M, Yaar M, Gilchrest BA. Cellular

mechanisms regulating human melanogenesis. Cell Mol Life Sci 2009; 66:1493–506.

8. Cui R, Widlund HR, Feige E, Lin JY, Wilensky DL, Igras VE, et al. Central role of p53 in the suntan response and pathologic hyperpigmentation. Cell 2007; 128:853–64.

9. Yang G, Li Y, Nishimura EK, Xin H, Zhou A, Guo Y, et al. Inhibition of PAX3 by TGF-beta modulates melanocyte viability. Mol Cell 2008; 32:554–63.

10. Goldstein NB, Koster MI, Hoaglin LG, Spoelstra NS, Kechris KJ, Robinson SE, et al. Narrow band ultraviolet B treatment for human vitiligo is associated with proliferation, migration, and differentiation of melanocyte precursors. J Invest Dermatol 2015; 135:2068–76.

11. Nishimura EK. Melanocyte stem cells: a melanocyte reservoir in hair follicles for hair and skin pigmentation. Pigment Cell Melanoma Res 2011; 24:401–10.

12. Nishimura EK, Granter SR, Fisher DE. Mechanisms of hair graying: incomplete melanocyte stem cell maintenance in the niche. Science 2005; 307:720–4.

13. He S, Yoon HS, Suh BJ, Eccles MR. PAX3 Is extensively expressed in benign and malignant tissues of the melanocytic lineage in humans. J Invest Dermatol 2010; 130:1465–8.

14. Medic S, Ziman M. PAX3 across the spectrum: from melanoblast to melanoma. Crit Rev Biochem Mol Biol 2009; 44:85–97.

15. Medic S, Ziman M. PAX3 expression in normal skin melanocytes and melanocytic lesions (naevi and melanomas). PLoS One 2010; 5:e9977.

16. Nonaka D, Chiriboga L, Rubin BP. Sox10: a pan-schwannian and melanocytic marker. Am J Surg Pathol 2008; 32:1291–8.

17. Shin J, Vincent JG, Cuda JD, Xu H, Kang S, Kim J, et al. Sox10 is expressed in primary melanocytic neoplasms of various histologies but not in fibrohistiocytic proliferations and histiocytoses. J Am Acad Dermatol 2012; 67:717–26.

18. Kubic JD, Young KP, Plummer RS, Ludvik AE, Lang D. Pigmentation PAX-ways: the role of Pax3 in melanogenesis, melanocyte stem cell maintenance, and disease. Pigment Cell Melanoma Res 2008; 21:627–45.

19. Lang D, Lu MM, Huang L, Engleka KA, Zhang M, Chu EY, et al. Pax3 functions at a nodal point in melanocyte stem cell differentiation. Nature 2005; 433:884–7.

20. Harris ML, Buac K, Shakhova O, Hakami RM, Wegner M, Sommer L, et al. A dual role for SOX10 in the maintenance of the postnatal melanocyte lineage and the differentiation of melanocyte stem cell progenitors. PLoS Genet 2013; 9:e1003644.

21. Hodgkinson CA, Moore KJ, Nakayama A, Steingrimsson E, Copeland NG, Jenkins NA, et al. Mutations at the mouse microphthalmia locus are associated with defects in a gene encoding a novel basic-helix-loop-helix-zipper protein. Cell 1993; 74:395–404.

22. King R, Weilbaecher KN, McGill G, Cooley E, Mihm M, Fisher DE. Microphthalmia transcription factor. A sensitive and specific melanocyte marker for melanoma diagnosis. Am J Pathol 1999; 155:731–8.

23. Costin GE, Hearing VJ. Human skin pigmentation: melanocytes modulate skin color in response to stress. FASEB J 2007; 21:976–94.

24. Cheli Y, Ohanna M, Ballotti R, Bertolotto C. Fifteen-year quest for microphthalmia-associated transcription factor target genes. Pigment Cell Melanoma Res 2010; 23:27–40.

25. McGill GG, Horstmann M, Widlund HR, Du J, Motyckova G, Nishimura EK, et al. Bcl2 regulation by the melanocyte master regulator Mitf modulates lineage survival and melanoma cell viability. Cell 2002; 109:707–18.

26. Bivik CA, Andersson EB, Rosdahl IK. Wavelength-specific effects on UVB-induced apoptosis in melanocytes. A study of Bcl-2/Bax expression and keratinocyte rescue effects. Melanoma Res 2005; 15:7–13.

27. Lopez-Camarillo C, Ocampo EA, Casamichana ML, Perez-Plasencia C, Alvarez-Sanchez E, Marchat LA. Protein kinases and transcription factors activation in response to UV-radiation of skin: implications for carcinogenesis. Int J Mol Sci 2012; 13:142–72.

28. Ho H, Aruri J, Kapadia R, Mehr H, White MA, Ganesan AK. RhoJ regulates melanoma chemoresistance by suppressing pathways that sense DNA damage. Cancer Res 2012; 72:5516–28.

29. Inomata K, Aoto T, Binh NT, Okamoto N, Tanimura S, Wakayama T, et al. Genotoxic stress abrogates renewal of melanocyte stem cells by triggering their differentiation. Cell 2009; 137:1088–99.

30. Murase D, Hachiya A, Amano Y, Ohuchi A, Kitahara T, Takema Y. The essential role of p53 in hyperpigmentation of the skin via regulation of paracrine melanogenic cytokine receptor signaling. J Biol Chem 2009; 284:4343–53.

31. Grichnik JM, Ali WN, Burch JA, Byers JD, Garcia CA, Clark RE, et al. KIT expression reveals a population of precursor melanocytes in human skin. J Invest Dermatol 1996; 106:967–71.

32. Hou L, Pavan WJ. Transcriptional and signaling regulation in neural crest stem cell-derived melanocyte development: do all roads lead to Mitf? Cell Res 2008; 18:1163–76.

33. Nishimura EK, Suzuki M, Igras V, Du J, Lonning S, Miyachi Y, et al. Key roles for transforming growth factor beta in melanocyte stem cell maintenance. Cell Stem Cell 2010; 6:130–40.

34. Prescribing, recording and reporting photon beam therapy (Report 50). Bethesda: International Commission on Radiation Units and Measurements; 1993.

35. Barlow JO, Maize J, Sr., Lang PG. The density and distribution of melanocytes adjacent to melanoma and nonmelanoma skin cancers. Dermatol Surg 2007; 33:199–207.

36. Kulesz-Martin M, Lagowski J, Fei S, Pelz C, Sears R, Powell MB, et al. Melanocyte and keratinocyte carcinogenesis: p53 family protein activities and intersecting mRNA expression profiles. J Investig Dermatol Symp Proc 2005; 10:142–52.

37. Bowen AR, Hanks AN, Allen SM, Alexander A, Diedrich MJ, Grossman D. Apoptosis regulators and responses in human melanocytic and keratinocytic cells. J Invest Dermatol 2003; 120:48–55.

38. Agresti A. Analysis of ordinal categorical data. Oxford: Wiley-Blackwell; 2010.

39. Team RC. R: A language and environment for statistical computing. Vienna: R Foundation for Statistical Computing; 2015.

40. Turesson I, Bernefors R, Book M, Flogegard M, Hermansson I, Johansson KA, et al. Normal tissue response to low doses of radiotherapy assessed by molecular markers–a study of skin in patients treated for prostate cancer. Acta Oncol 2001; 40:941–51.

41. Pellegrini G, Dellambra E, Golisano O, Martinelli E, Fantozzi I, Bondanza S, et al. p63 identifies keratinocyte stem cells. Proc Natl Acad Sci U S A 2001; 98:3156–61.

42. Senoo M, Pinto F, Crum CP, McKeon F. p63 Is essential for the proliferative potential of stem cells in stratified epithelia. Cell 2007; 129:523–36.

43. Truong AB, Kretz M, Ridky TW, Kimmel R, Khavari PA. p63 regulates proliferation and differentiation of developmentally mature keratinocytes. Genes Dev 2006; 20:3185–97.

44. Yang A, Schweitzer R, Sun D, Kaghad M, Walker N, Bronson RT, et al. p63 is essential for regenerative proliferation in limb, craniofacial and epithelial development. Nature 1999; 398:714–8.

45. Brinck U, Ruschenburg I, Di Como CJ, Buschmann N, Betke H, Stachura J, et al. Comparative study of p63 and p53 expression in tissue microarrays of malignant melanomas. Int J Mol Med 2002; 10:707–11.

46. de la Serna IL, Ohkawa Y, Higashi C, Dutta C, Osias J, Kommajosyula N, et al. The microphthalmia-associated transcription factor requires SWI/SNF enzymes to activate melanocyte-specific genes. J Biol Chem 2006; 281:20233–41.

47. Tadokoro T, Yamaguchi Y, Batzer J, Coelho SG, Zmudzka BZ, Miller SA, et al. Mechanisms of skin tanning in different racial/ethnic groups in response to ultraviolet radiation. J Invest Dermatol 2005; 124:1326–32.

48. Fitzpatrick TB. The validity and practicality of sun-reactive skin types I through VI. Arch Dermatol 1988; 124:869–71.

49. Roberts WE. Skin type classification systems old and new. Dermatol Clin 2009; 27:529–33, viii.

50. Hornyak TJ, Jiang S, Guzman EA, Scissors BN, Tuchinda C, He H, et al. Mitf dosage as a primary determinant of melanocyte survival after ultraviolet irradiation. Pigment Cell Melanoma Res 2009; 22:307–18.

51. Park JH, Park EJ, Hur SK, Kim S, Kwon J. Mammalian SWI/SNF chromatin remodeling complexes are required to prevent apoptosis after DNA damage. DNA Repair (Amst) 2009; 8:29–39.

52. Gupta PB, Kuperwasser C, Brunet JP, Ramaswamy S, Kuo WL, Gray JW, et al. The melanocyte differentiation program predisposes to metastasis after neoplastic transformation. Nat Genet 2005; 37:1047–54.

53. Rudolph P, Tronnier M, Menzel R, Moller M, Parwaresch R. Enhanced expression of Ki-67, topoisomerase IIalpha, PCNA, p53 and p21WAF1/Cip1 reflecting proliferation and repair activity in UV-irradiated melanocytic nevi. Hum Pathol 1998; 29:1480–7.

54. Wang XD, Morgan SC, Loeken MR. Pax3 stimulates p53 ubiquitination and degradation independent of transcription. PLoS One 2011; 6:e29379.

55. Kemp MG, Sancar A. ATR kinase inhibition protects non-cycling cells from the lethal effects of dna damage and transcription stress. J Biol Chem 2016; 291:9330–42.

56. Bakkenist CJ, Kastan MB. DNA damage activates ATM through intermolecular autophosphorylation and dimer dissociation. Nature 2003; 421:499–506.